Biochimica et Biophysica Acta 1798 (2010) 569–578

Contents lists available at ScienceDirect

Biochimica et Biophysica Acta

journal homepage: www.elsevier.com/locate/bbamem

Regulation by CRAMP of the responses of murine peritoneal macrophages to extracellular ATP☆

Michèle Seil [a], Elie Kabré [b], Carole Nagant [a], Michel Vandenbranden [c], Unai Fontanils [d], Aida Marino [d], Stéphanie Pochet [a], Jean-Paul Dehaye [a,*]

[a] Laboratoire de Chimie biologique et médicale et de Microbiologie pharmaceutique, Institut de Pharmacie C.P. 205/3, Université libre de Bruxelles, Bruxelles, Belgium
[b] Laboratoire de Biochimie et d'Immunologie, Unité de Formation et de Recherche des Sciences de la Santé, Université de Ouagadougou, Burkina Faso
[c] Laboratory for the Structure and Function of Biological Membranes, Center for Structural Biology and Bioinformatics, Faculty of Sciences C.P. 206/02, Université libre de Bruxelles, Bruxelles, Belgium
[d] Departamento de Bioquímica y Biología Molecular, Facultad de Ciencias, Universidad del Pais Vasco, 48080 Bilbao, Spain

ARTICLE INFO

Article history:
Received 11 September 2009
Received in revised form 27 October 2009
Accepted 4 November 2009
Available online 11 November 2009

Keywords:
Antimicrobial peptide
Purinergic receptor
$P2X_7$-KO mice
Ivermectin

ABSTRACT

Peritoneal macrophages were isolated from wild type (WT) mice and from mice invalidated for the $P2X_7$ receptor (KO) which had been pretreated with thioglycolate. In cells from WT mice, 1 mM ATP increased the intracellular concentration of calcium ($[Ca^{2+}]_i$), the uptake of ethidium bromide, the production of reactive oxygen species (ROS), the secretion of IL-1β, the release of oleic acid and of lactate dehydrogenase; it decreased the intracellular concentration of potassium ($[K^+]_i$). In KO mice, ATP transiently increased the $[Ca^{2+}]_i$ confirming that the $P2X_7$ receptor is a major receptor of peritoneal macrophages. WKYMVm, an agonist of receptors for formylated peptides (FPR) also increased the $[Ca^{2+}]_i$ in murine macrophages. The slight increase of the $[Ca^{2+}]_i$ was strongly potentiated by ivermectin confirming the expression of functional $P2X_4$ receptors by murine peritoneal macrophages. CRAMP, the unique antimicrobial peptide derived from cathelin in mouse inhibited all the responses coupled to $P2X_7$ receptors in macrophages from WT mice. Agonists for FPR had no effect on the increase of the $[Ca^{2+}]_i$ in response to ATP. CRAMP had no effect on the increase of the $[Ca^{2+}]_i$ evoked by a combination of ATP and ivermectin in macrophages from $P2X_7$-KO mice. In summary CRAMP inhibits the responses secondary to the activation of the murine $P2X_7$ receptors expressed by peritoneal macrophages. This inhibition is not mediated by FPR receptors and is specific since CRAMP has no effect on the response coupled to $P2X_4$ receptors. It can thus be concluded that the interaction between $P2X_7$ receptors and cathelin-derived antimicrobial peptides is species-specific, in some cases (man) positive in others (mouse) negative.

1. Introduction

Cathelicidins are proteins related to the cationic host defense peptides and contribute to the primary, innate phase of immunity [1]. They are expressed by macrophages, lymphocytes, epithelial cells, keratinocytes, cells lining the upper respiratory tree, vaginal cells. Their conserved N-terminal domain shares analogies with cathelin, an inhibitor of cathepsin L. Consensus sequences for proteases are present in the central domain of these proteins. The sequence of the C-terminal domain varies according to species from 12 to more than 100 residues [2]. After their release in the extracellular medium, cathelicidins are digested by elastase or proteinase 3 or kallikrein and their C-terminal domain which is a peptide with bactericidal properties is released [3]. LL-37 is the sole human orthologue of these peptides and is derived from an 18-kDa precursor [4]. Its unusually high content of basic and hydrophobic residues accounts for its ability to form an amphipathic alpha helix [5]. LL-37 interacts with the negative charges surrounding bacteria through the positively charged side of the helix. In a second step the hydrophobic residues of the peptide affect the structure and the integrity of the membrane of the bacteria, a process which eventually kills them. These bactericidal properties of LL-37 are very sensitive to the ionic composition of the medium specially the concentration of cations. In media with an ionic

Abbreviations: a.f.u., arbitrary fluorescence units; ATR-FTIR, attenuated total reflection–Fourier transform infrared spectroscopy; BSA, bovine serum albumin; CRAMP, cathelin-related antimicrobial peptide; DCFH-DA, 2′,7′-dichlorodihydrofluorescein diacetate; EGTA, ethylene glycol-*bis*-(β-aminoethyl ether)-*N*,*N*,*N*′,*N*′-tetraacetic acid; FBS, fetal bovine serum; FPR, receptors for formylated peptides; HEPES, *N*-[2-hydroxyethyl] piperazine-*N*′-[2-ethanesulfonic acid]; KO mice, knockout mice; ROS, reactive oxygen species; WT mice, wild-type mice

☆ This work was supported by grant n° 3.4.528.07.F from the Fonds National de la Recherche Scientifique to S. Pochet and J.P. Dehaye and by grant BFU/2007-62728/BMC from MEC to A. Marino. S. Pochet was a postdoctoral researcher of the Fonds National de la Recherche Scientifique, E. Kabré was supported by a postdoctoral grant from the Commission Universitaire pour le Développement de Belgique, M. Vandenbranden is supported by the Fonds National de la Recherche Scientifique and U. Fontanils by a fellowship from the University of the Basque Country.

* Corresponding author.
E-mail address: jdehaye@ulb.ac.be (J.-P. Dehaye).

0005-2736/$ – see front matter © 2009 Elsevier B.V. All rights reserved.
doi:10.1016/j.bbamem.2009.11.002

composition similar to our extracellular milieu the concentrations of LL-37 required to observe a bactericidal effect are so high that the bactericidal activity in vivo has been questioned [6]. LL-37 has many other effects [7]. It is chemotactic for macrophages, neutrophils and polymorphonuclear leukocytes and it promotes the degranulation of mast cells [8], it accelerates wound healing [9] and increases angiogenesis [10]. It also neutralizes LPS activity [11]. These pleiotropic responses involve various receptors such as Toll like receptors [12], epidermal growth factor receptor [13] or receptors for formylated peptides (FPR) [14]. Recently Mookherjee et al. [15] reported that the immunomodulatory functions of LL-37 were mediated by an intracellular receptor, the glyceraldehyde 3-phosphate dehydrogenase (GPDH). More relevant to the present work, Elssner et al [16] showed that LL-37 could increase the release of IL-1β from human macrophages. This response was blocked by antagonists of the $P2X_7$ receptor suggesting that LL-37 could activate this purinergic receptor in macrophages. The affinity of the $P2X_7$ receptor for ATP is very low (in the millimolar range) and it is very unlikely that after its diffusion in the extracellular medium such high concentrations of the nucleotide reach the $P2X_7$ receptor expressed in the plasma membrane of a neighbor cell. Considering that low concentrations of LL-37 could stimulate this receptor, it was suggested that the $P2X_7$ receptor was more a receptor for antimicrobial peptides than for adenine nucleotides. At the opposite with this general view, Mookherjee et al. [15] have reported that inhibitors of $P2X_7$ receptors had no effect on the secretion of MCP-1 from monocytes stimulated by LL-37. We have previously reported that LL-37 inhibited the $P2X_7$ receptor expressed by mouse submandibular glands [17]. Since this result could be explained either by a species (man versus mouse) or a tissue (macrophage versus exocrine gland) difference, we decided to reevaluate the response of murine macrophages to CRAMP, the unique cathelicidin expressed by mice [18]. Our results show that CRAMP inhibits the responses coupled to $P2X_7$ receptors (calcium uptake, potassium release, formation of reactive oxygen species (ROS), release of oleic acid, secretion of IL-1β, uptake of ethidium bromide and release of LDH) without affecting the variation of the $[Ca^{2+}]_i$ in response to the activation of $P2X_4$ receptors. The mouse $P2X_7$ receptor is thus the target of CRAMP, the murine antimicrobial cathelicidin-related peptide. The interaction between CRAMP and the purinergic receptor provokes the inhibition, not the activation of the receptor. It is thus concluded that, at least in mouse, the cathelicidin-related peptide is not the natural agonist of $P2X_7$ receptors.

2. Materials and methods

2.1. Materials

Ethylene glycol-*bis*-(β-aminoethyl ether)-*N*,*N*,*N*',*N*'-tetraacetic acid (EGTA), *N*-[2-hydroxyethyl] piperazine-*N*'-[2-ethanesulfonic acid] (HEPES), ivermectin, adenosine 5′-triphosphate disodium salt (ATP), fetal bovine serum (FBS), lipopolysaccharide from *E. coli* (LPS, Sigma catalog ref. 2880), β-NADH, sodium pyruvate and formylated Met-Leu-Phe (fMLF) were obtained from Sigma-Aldrich (St. Louis, MO). Bovine serum albumin (BSA) fraction V was from Roche Diagnostics (Mannheim, Germany). Trishydroxymethylaminomethane (TRIS) was from VWR (Leuven, Belgium). GLLRKGGEKIGEKLKKIGQKIKNFFQKLVPQPEQ (CRAMP), LESIFRSLLFRVM (MMK-1), Try-Lys-Tyr-Met-Val-D-Met-NH_2 (WKYMVm) and KRIVQRIKDFLRNLVPRTES (KR-20) were custom synthesized with 99% purity by GL Biochem (Shanghai, China). 9,10-[^{3}H]oleic acid was purchased from American Radiolabeled Chemicals Inc. (St. Louis, MO). The scintillation solution Ecoscint A was from National Diagnostics (Atlanta, GA). The 2′,7′-dichlorodihydrofluorescein diacetate (DCFH-DA), fura2-AM, ethidium bromide, PBFI-AM, the glutamine-free amino acids mixture, phosphate-buffered saline (PBS), RPMI-1640, Hanks' balanced salt solution (HBSS), L-glutamine and the solution of penicillin–streptomycin were from Invitrogen (Groningen, The Netherlands). Thioglycollate was from Becton-Dickinson (Franklin Lanes, NJ). The polyclonal anti-mouse IL-1β antibody was from R&D Systems (Minneapolis, MN). The biotinylated monoclonal anti-mouse IL-1β antibody and the mouse IL-1β were from Endogen (Perbio Science, Erembodegem, Belgium). The HRP substrate 1 Step Ultra TMB-ELISA and the peroxidase-linked streptavidin were from Pierce (Perbio Science, Erembodegem, Belgium).

The experiments were carried out on C57Bl/6J $P2X_7R^{+/+}$ wild-type mice (WT) and $P2X_7R^{-/-}$ null mice (KO) kindly supplied by Pfizer Inc. (Groton, CT). Breeding of $P2X_7$ knockout mice males with females was used to maintain the colony of receptor-deficient animals. Mice used in the experiments were between 20 and 25 g. The expression of $P2X_7$ receptors in wild-type mice and its absence in null mice was tested by Western blot as previously described [19].

2.2. Cell culture

Adult male WT or KO mice (25 g) were used for these experiments. Peritoneal macrophages were prepared according to McCarron et al. [20]. Briefly, peritoneal exsudates were induced by injection of 1.5 ml thioglycollate solution (4% in sterile water) 3 or 4 days before harvesting the cells. The animals were fasted overnight and sacrificed by rising the CO_2 concentration in accordance with the procedures of the Belgian Ministry of Agriculture under the supervision of the institutional ethical committee (protocol no. 221N). Ten milliliters of sterile phosphate-buffered saline (PBS) without calcium or magnesium (pH 7.2) containing 10 U/ml heparin were injected in the peritoneal cavity. The abdomen was gently massaged after its distension. The fluid was recovered and transferred to a sterile tube kept on ice. After centrifugation at 1500 g for 10 min at 4 °C, the cellular pellet was resuspended in RPMI 1640 medium supplemented with 20 mM HEPES, 10% fetal bovine serum (FBS), 2 mM L-glutamine, 100 U/ml penicillin and 100 μg/ml streptomycin (RPMI medium). Ten million cells were added to culture flasks (usually two flasks per mouse) and incubated at 37 °C for at least 2 h in a humidified atmosphere containing 5% CO_2. Nonadherent cells and the medium were then aspirated and replaced with 10 ml fresh RPMI medium. The cells were incubated overnight at 37 °C in the presence of 250 ng/mL LPS before use.

2.3. Determination of the $[Ca^{2+}]_i$

The culture plates were washed twice with 10 ml PBS. The cells were gently scraped off the plates with a rubber policeman. They were incubated at 25 °C for at least 1 h in a HEPES-buffered medium (HBM) containing (mM): 24.5 HEPES (pH 7.4), 96 NaCl, 6 KCl, 2.5 NaH_2PO_4, 11.5 glucose, 5 sodium pyruvate, 5 sodium glutamate, 5 sodium fumarate. This medium also contained 1 mM $CaCl_2$ and $MgCl_2$, 1% (v/v) glutamine-free amino acids mixture, 1% (w/v) BSA (medium HBT) in the presence of 3 μM fura2-AM. At the end of this incubation the cells were washed and diluted with HBM supplemented with 1 mM $CaCl_2$. They were transferred in the cuvette of a fluorimeter and maintained at 25 °C under constant stirring. The light emitted at 510 nm was measured after excitation at 340 and 390 nm. At the end of the incubation, the cells were permeabilized with 100 μM digitonin and the autofluorescence of the samples was estimated by quenching of fura2 with 100 mM manganese. The blank values were subtracted from the results and the $[Ca^{2+}]_i$ was estimated as described by Grynkiewicz et al. [21].

2.4. Determination of the $[K^+]_i$

Macrophages were incubated at 25 °C for at least 1 h in HBT in the presence of 3 μM PBFI-AM. At the end of this incubation, the cells were

washed and diluted with HBM medium with 1 mM $CaCl_2$. They were transferred in the cuvette of a fluorimeter and maintained at 25 °C under constant stirring. The light emitted at 490 nm (slitwidth 16 nm) was measured after excitation at 345 nm (slitwidth 16 nm). Before the beginning of each measurement the voltage was adjusted to get a signal corresponding to 10% of the maximal signal. Results have been plotted as arbitrary fluorescence units (a.f.u.) without any attempt to calibrate the traces.

2.5. Assay of the formation of a pore

The cells were washed twice with 10 ml PBS and gently scraped off the plate with a rubber policeman. The formation of the pore was measured with the fluorescent dye ethidium bromide [22]. Macrophages from two mice were diluted with 3 ml HBT and for each assay, a 1-ml aliquot was washed and diluted with 2 ml HBM. Ethidium bromide was added at a final concentration of 20 μM. The cells were allowed to equilibrate for 5 min before the beginning of the measurement which was performed at 37 °C under constant stirring. The samples were excited at 360 nm and the light emitted at 580 nm was measured every second. At the end of the measurement, the maximum uptake was estimated by adding 100 μM digitonin and the results were calculated taking this value as reference.

2.6. Assay of the production of ROS

The production of ROS was estimated with 2′,7′-dihydrodichlorofluorescein (DCFH) which becomes fluorescent after oxidation to 2′,7′-dichlorofluorescein (DCF) by hydrogen peroxide, peroxyl radical or peroxynitrite anion [23]. Aliquots (1 ml) of the cellular suspension were preincubated in the dark, at 25 °C for at least 1 h in HBT in the presence of 6 μM DCFH-DA, a cell-permeant analog of DCFH. After this incubation, 0.5 ml of the cellular suspension were washed once with NaCl 0.9% and the cellular pellet was resuspended in 2 ml HBM with 1 mM calcium. The assay was performed at 25 °C under constant stirring in the cuvette of a fluorimeter. The samples were excited at 485 nm and the light emitted at 525 nm was measured every second.

2.7. Assay of IL-1β secretion

Peritoneal macrophages from one mouse were resuspended in RPMI medium and plated at 500,000 cells/ml in 12-well plates. After 3 h at 37 °C, the medium was removed and the cells were incubated overnight in fresh RPMI medium containing 250 ng/ml LPS. The cells were washed twice with PBS. They were then incubated for 15 min at 37 °C in 1 ml Hanks' balanced salt solution (HBSS) without magnesium but containing 1 mM $CaCl_2$, 0.1% BSA and the tested agent. Each condition was tested in duplicates. Incubation medium was collected and centrifuged at 10,000 *g* for 5 min to remove detached cells. The IL-1β content was assayed by sandwich ELISA. A 96-well plate was coated overnight with 1 μg/ml polyclonal anti-mouse IL-1β antibody and blocked with 4% BSA in PBS for 1 h at room temperature. The wells were washed twice with Tris–Tween buffer (Tris–HCl 50 mM, pH 7.5 and 0.2% Tween-20). Aliquots of medium samples or recombinant IL-1β standards were diluted to 150 μl with HBSS containing 1 mM $CaCl_2$ and 0.1% BSA and mixed with 150 μL biotinylated monoclonal anti-mouse IL-1β antibody (0.4 μg/ml solution). One hundred microliters of this mix was added in duplicate to the wells. Each assay was performed in duplicates. The plate was incubated at 37 °C for 2 h and then washed four times. The captured immune complexes were incubated for 30 min at room temperature with 100 μL streptavidin-HRP (0.2 μg/mL), washed four times and colorimetrically developed with 100 μL HRP substrate. After the addition of 100 μL stop solution (H_2SO_4 1.8 M), the absorbance was read at 450 nm in a Synergy HT plate reader (Bio-Tek, Winooski, VT).

2.8. Assay of the release of oleic acid

Peritoneal macrophages from three mice were diluted with RPMI medium and plated. After 3 h at 37 °C, the medium was removed and the cells were incubated overnight in RPMI medium containing 0.5 μCi/ml [^{3}H]oleic acid. The medium was removed and the cells were washed twice with 10 ml PBS. They were then incubated for 1 h at room temperature in RPMI medium. After two washes with PBS, the cells were incubated in 1 ml HBM supplemented with 0.1% BSA, the amino acid mixture and 1 mM $CaCl_2$ and the tested agent for 20 min at 37 °C. Each assay was performed in triplicate. At the end of the incubation, 600 μl of the supernatant were centrifuged for 5 min at 10,000 *g* to remove detached cells and 500 μl were transferred to scintillation vials. The radioactivity was estimated in a TriCarb liquid scintillation analyzer (Perkin Elmer, Waltham, MA) after the addition of 5 ml Ecoscint A (National Diagnostics, Atlanta, GA).

2.9. Assay of the release of LDH

Macrophages were resuspended in HBM medium supplemented with 0.1% BSA, 1% (v/v) glutamine-free amino acids and 1 mM $CaCl_2$, in the absence of magnesium. They were incubated at 37 °C under constant agitation either in control or in the tested condition. Each condition was tested in triplicate. At the end of the incubation the cellular suspension was centrifuged for 5 min at 10,000×*g*. To estimate the amount of LDH present in the medium at the beginning of the incubation (blank values), a similar procedure was applied to non-incubated aliquots of cells. Aliquots of cells were also sonicated to estimate the total LDH activity. The assay was performed in a 96-well microplate. Ten microliters of the enzyme solution (cellular supernatant) were transferred to the wells. Then, 190 μl of Tris–EGTA–NADH (56 mM Tris, pH 7.4, 5.6 mM EGTA and 170 μM β-NADH) and 20 μl of 14 mM pyruvate were added to the wells. The disappearance of NADH was monitored at 340 nm for 20 min at 30 °C (Synergy HT, BioTek). Absorbance measurements were performed at time intervals of 45 s, the absorbance decreasing linearly with time. The change of absorbance per minute was calculated by linear regression and the blank value was subtracted from the results obtained with the incubated cells.

2.10. Determination of the secondary structure of CRAMP using attenuated total reflection–Fourier transform infrared spectra (ATR-FTIR)

KR-20 was dissolved in 2 mM HEPES and CRAMP in DMSO at a 5 mg/ml concentration. Just before measurement, 2 μl CRAMP were deposited on a 0.025-μm pore size dialysis disc (Millipore VSWP02500) floating on 2 mM HEPES buffer solution (pH 7.4). After 10 min, the dialyzed sample was transferred to the ATR reflect. The infrared spectra were obtained and analyzed as described in ref. [24]. Briefly 1 μl of the peptide solution (KR-20 or dialyzed CRAMP) were uniformally spread on a diamond internal reflection element. The samples were evaporated under a stream of nitrogen. The spectra were obtained on a Bruker IFS55 FTIR spectrophotometer (Bruker, Ettlingen, Germany) equipped with a MCT detector (broadband 120,000–420 cm^{-1}, liquid nitrogen cooled) at a resolution of 2 cm^{-1} and were subtracted for residual water vapor spectral contribution to the signal. The amide hydrogen/deuterium exchange was performed as described by Vigano et al. [25]. Briefly the sample was flushed with nitrogen gas saturated with D_2O by bubbling through a series of four vials containing D_2O. Exchange was monitored by the decrease of the amide II peak area around

1550 cm^{-1} which is sensitive to H/D exchange as compared with the amide I peak area (1600–1700 cm^{-1} region) taken as a reference. The spectra obtained after deuteration were analyzed by Fourier self-deconvolution as previously described [25].

2.11. Statistical analysis

Results were analyzed with the Mann–Whitney non-parametric test. $^{***}P<0.001$; $^{**}P<0.01$; $^{*}P<0.05$.

3. Results

3.1. Effect of CRAMP on the variation of the $[Ca^{2+}]_i$ in response to extracellular ATP

The murine peritoneal macrophages were detached from the culture plate and loaded with fura2. The $[Ca^{2+}]_i$ was measured in the presence of 1 mM calcium but in the absence of extracellular magnesium. As shown in Fig. 1, the $[Ca^{2+}]_i$ was rather stable when the macrophages were incubated in control conditions at 25 °C. The addition of 1 mM ATP sharply increased the $[Ca^{2+}]_i$ (from 97 ± 8 nM to 486 ± 54 nM within 10 s) which nearly doubled for the next 3 min. By itself CRAMP (1–10 μM concentration range) did not significantly affect the $[Ca^{2+}]_i$. The peptide dose-dependently inhibited the late response to extracellular ATP (from 733 ± 75 nM without CRAMP down to 336 ± 39 nM with CRAMP 3 min after the addition of ATP) without affecting the rapid increase of the $[Ca^{2+}]_i$ (486 ± 54 nM without CRAMP versus 494 ± 50 nM with CRAMP 10 s after the addition of ATP). The variation of the $[Ca^{2+}]_i$ 30 s before and 1 min after the addition of ATP to the medium was plotted as a function of the concentration of CRAMP (Fig. 1). The half maximal inhibitory concentration of CRAMP ranged between 300 nM and 1 μM. These results suggested that CRAMP inhibited one of the purinergic receptors expressed by macrophages.

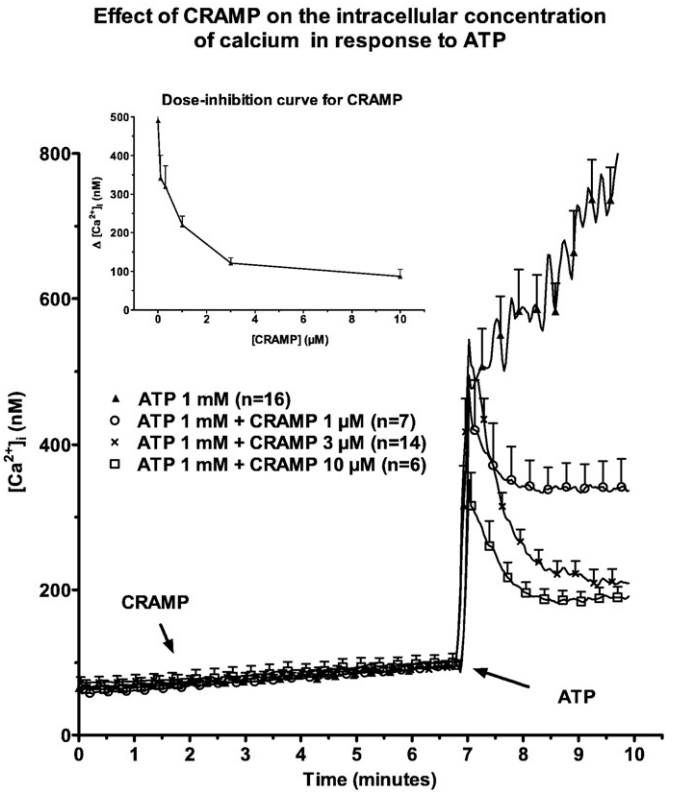

Fig. 1. Effect of CRAMP on the increase of the $[Ca^{2+}]_i$ in murine peritoneal macrophages exposed to ATP. Peritoneal macrophages loaded with fura2 were incubated at 25 °C in a medium containing 1 mM $CaCl_2$ in control conditions. At 2 min various concentrations of CRAMP were added to the medium. At 7 min the cells were exposed to 1 mM ATP. Results are expressed as the $[Ca^{2+}]_i$ and are the means ± S.E.M. of *n* experiments. For the clarity of the graph only one out of every 10 points has been plotted. *Insert*: The variation of the $[Ca^{2+}]_i$ 30 s before and 1 min after the addition of 1 mM ATP was plotted as a function of the concentration of CRAMP.

3.2. Interaction between CRAMP and the ATP-gated cation channel

In the next experiments the effect of the peptide on the uptake of extracellular calcium was tested (Fig. 2, lower panel). Calcium (1 mM) was added to the medium of cells preincubated in the presence of EGTA. In control cells calcium provoked a rapid and transient increase of the $[Ca^{2+}]_i$. In cells stimulated with 1 mM ATP the addition of calcium to the medium provoked a more substantial initial increase of the $[Ca^{2+}]_i$ followed by a sustained increase for the next 5 min. CRAMP had no effect on the basal uptake of calcium, but in the presence of 1 mM ATP it inhibited part of the initial increase and fully suppressed the sustained uptake in response to the nucleotide. These results suggested that ATP activated a P2X receptor coupled to a calcium channel which remained open for several minutes and which was blocked by CRAMP. Among P2X receptors macrophages mostly express $P2X_4$ and $P2X_7$ receptors [26]. To determine which of these receptors was regulated by

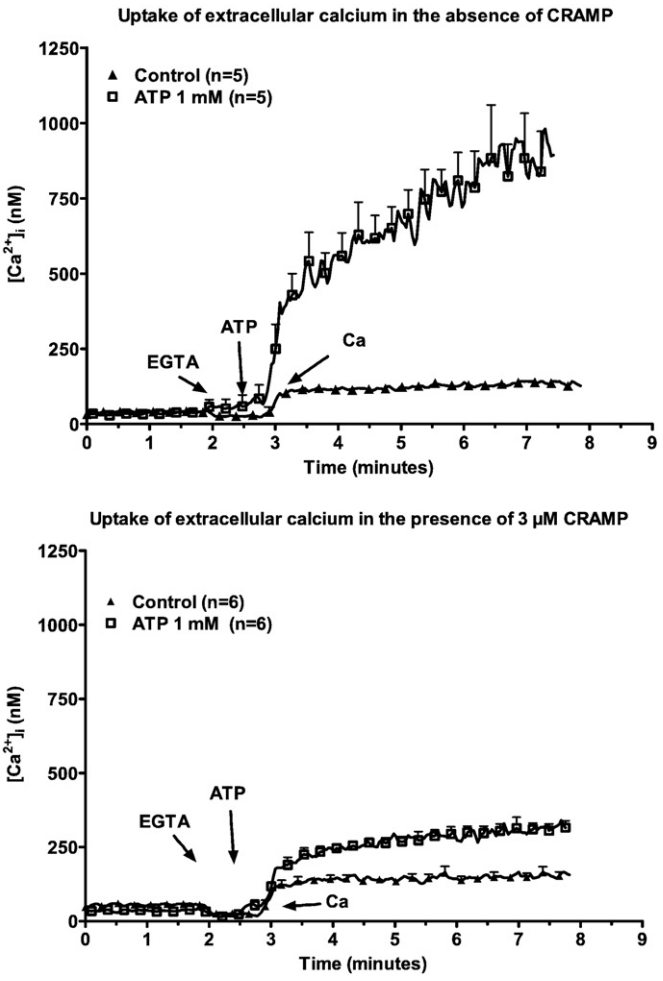

Fig. 2. Effect of CRAMP on the uptake of extracellular calcium in response to 1 mM ATP. Peritoneal macrophages loaded with fura2 were incubated at 25 °C in the absence (upper panel) or in the presence (lower panel) of 3 μM CRAMP, in the absence of extracellular calcium. Two minutes after the beginning of the assay, 100 μM EGTA was added to the medium followed 30 s later by 1 mM ATP. At 3 min calcium was added to the medium at a final 1 mM concentration. Results are the means ± S.E.M. of *n* experiments.

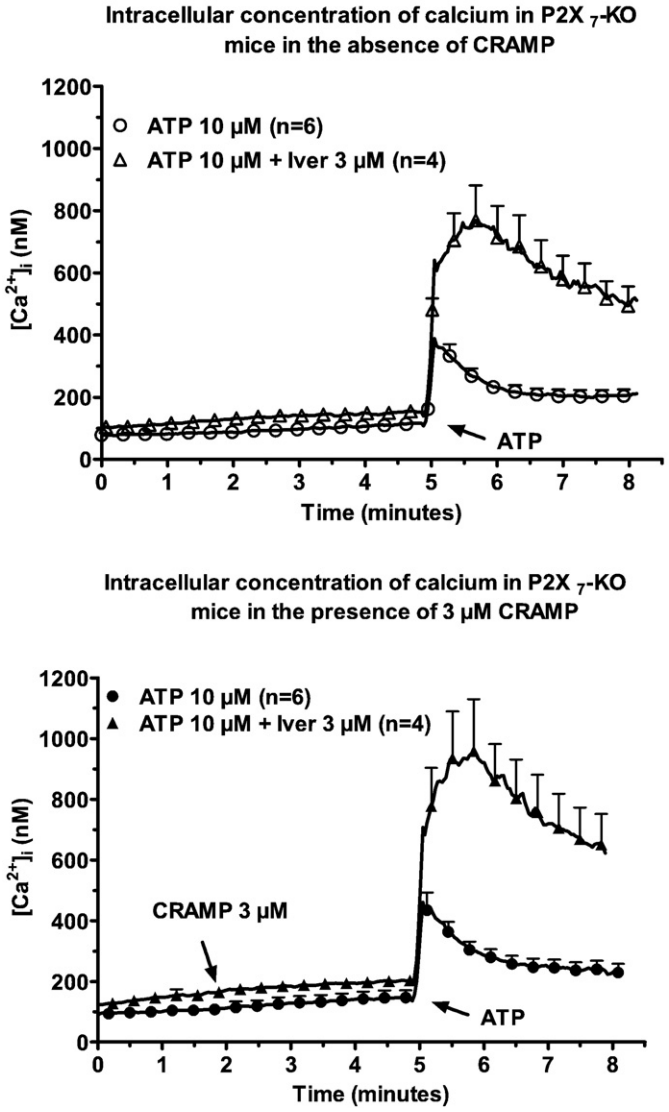

Fig. 3. Effect of CRAMP on the variation of the $[Ca^{2+}]_i$ in macrophages from $P2X_7$-KO mice in response to ATP. Peritoneal macrophages from $P2X_7$-KO mice were incubated at 25 °C in the presence of 1 mM $CaCl_2$; in the absence (circles) or in the presence of 3 μM ivermectin (triangles). Two minutes after the beginning of the assay CRAMP was added to the medium at a 3-μM final concentration (closed symbols). Three minutes later the cells were stimulated with 10 μM ATP. The results are the means ± S.E.M. of *n* experiments.

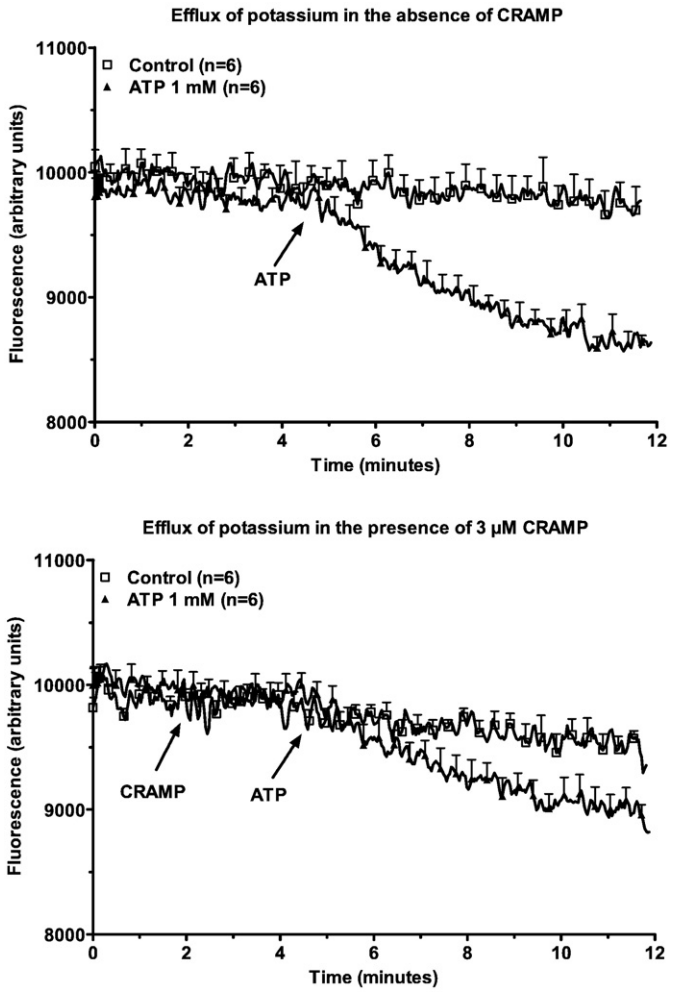

Fig. 4. Effect of CRAMP on the variation of the $[K^+]_i$ in response to ATP. Peritoneal macrophages loaded with PBFI were incubated at 25 °C in the presence of 1 mM $CaCl_2$. Two minutes after the beginning of the assay CRAMP was added to the medium at a 3-μM final concentration (lower panel). Three minutes later some cells were stimulated with 1 mM ATP (triangles). Results are the means ± S.E.M. of *n* experiments.

CRAMP the next experiments were performed with macrophages from $P2X_7$-KO mice. We have previously confirmed that these mice do not express $P2X_7$ receptors [19]. As shown in the upper panel of Fig. 3, a low concentration of ATP (10 μM) provoked a slight and transient increase of the $[Ca^{2+}]_i$ in the macrophages from $P2X_7$-KO mice. Ivermectin is a macrolide which potentiates the responses coupled to the $P2X_4$ receptor by blocking its internalization on one hand and by its interaction with an allosteric site on the other hand [27]. When cells were preincubated with ivermectin, the variation of the $[Ca^{2+}]_i$ in response to ATP was increased and prolonged (Fig. 3, upper panel). CRAMP had no effect on the response of macrophages from $P2X_7$-KO mice either to ATP alone or to ATP plus ivermectin suggesting that it did not block the channel coupled to $P2X_4$ receptors (Fig. 3, lower panel). The activation of $P2X_7$ receptors increases the permeability not only to calcium but also to potassium. Macrophages were loaded with PBFI which is a fluorescent dye sensitive to the concentration of potassium. The fluorescence did not vary in macrophages incubated in control conditions at 25 °C (Fig. 4). The addition of 1 mM ATP to the medium provoked a steady decrease of the signal. This drop disappeared when macrophages were incubated in the presence of a high (90 mM) concentration of potassium. CRAMP had, by itself, no effect on the fluorescence of PBFI confirming that it did not open the non-selective cation channel. The decrease of the fluorescence of PBFI in response to ATP was inhibited in cells incubated in the presence of 3 μM CRAMP. From these results it can be concluded that CRAMP inhibited the non-selective cation channel coupled to $P2X_7$ receptors.

3.3. Effect of agonists for FPR on the response to ATP

Cathelin-derived peptides activate receptors for chemotactic formylated peptides [14]. Considering that murine macrophages express some classes of these receptors [28], the inhibition exerted by CRAMP on the non-selective channel coupled to $P2X_7$ receptors might be secondary to its activation of chemotactic receptors. To test this hypothesis the interaction between ATP and other agonists of FPRs was examined. As shown in Fig. 5, 1 μM fMLF (a specific agonist for FPR) and 10 μM MMK-1 (a specific agonist for formylated peptide receptor like-1, FPRL1/FPR2) had by themselves no effect on the $[Ca^{2+}]_i$; 10 μM WKYMVm (a specific agonist for formylated peptide receptor like-2, FPRL2/FPR3) transiently doubled the $[Ca^{2+}]_i$ (from

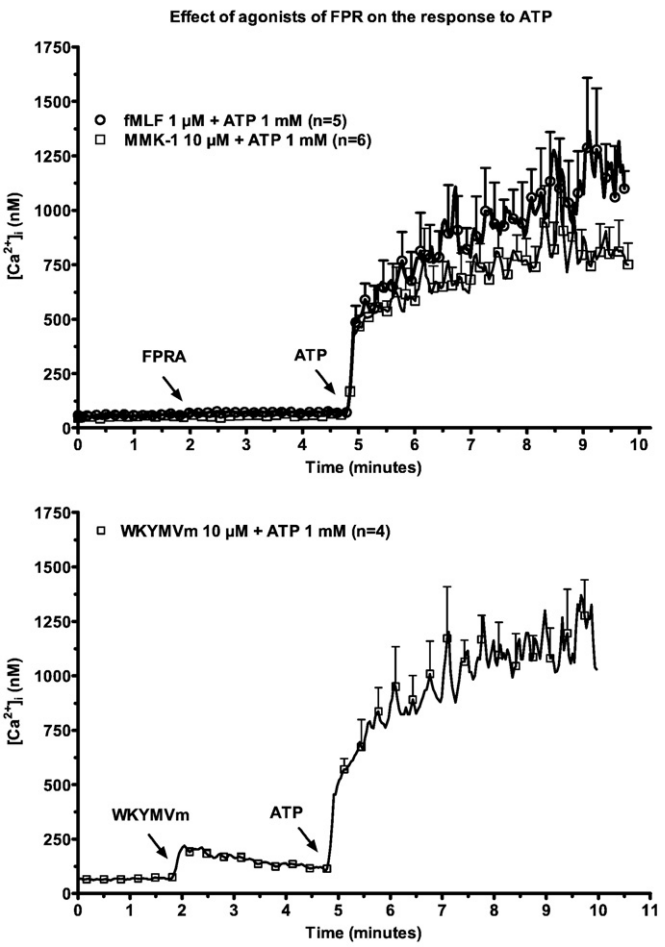

Fig. 5. Effect of agonists of formylated peptide receptors (FPR) on the variation of the $[Ca^{2+}]_i$ in response to ATP. Peritoneal macrophages loaded with fura2 were incubated at 25 °C in the presence of 1 mM $CaCl_2$. Two minutes after the start of the assay, the cells were exposed to an agonist of a receptor for formylated peptides (FPRA). Three minutes later 1 mM ATP was added to the medium. Results are the means ± S.E.M. of *n* experiments.

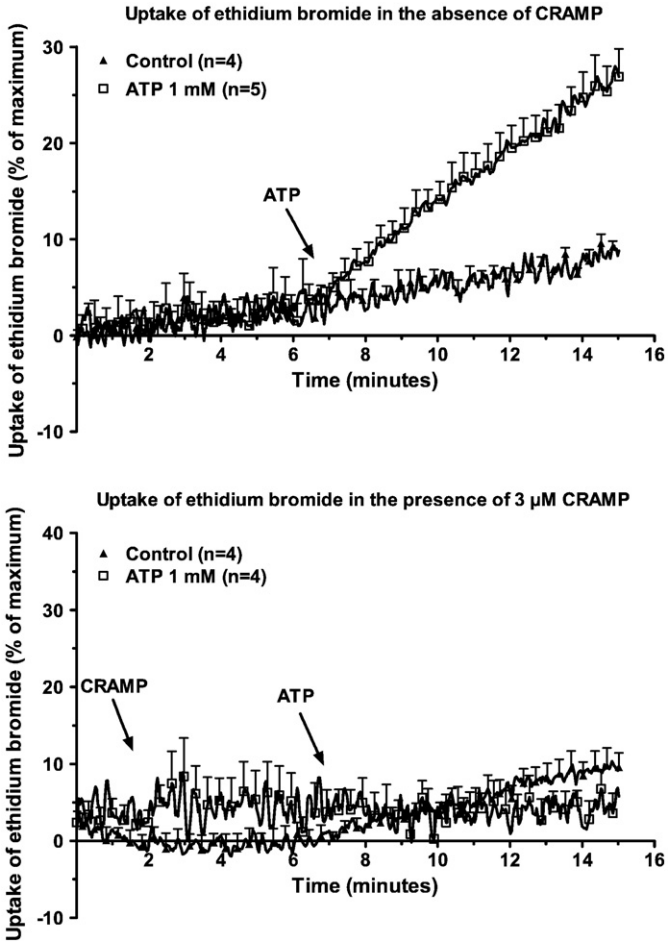

Fig. 6. Effect of CRAMP on the uptake of ethidium bromide in response to ATP. Peritoneal macrophages were incubated at 37 °C in the presence of ethidium bromide and in the absence of extracellular calcium. Two minutes after the start of the assay 3 μM CRAMP was added to the medium (lower panel) or the cells were maintained in control conditions (upper panel). Five minutes later some cells were exposed to 1 mM ATP (squares) and the other cells were incubated in control conditions (triangles). The results are expressed as the percentage of maximal uptake of ethidium bromide and are the means ± S.E.M. of *n* experiments. For the clarity of the graph only 1 out of every 15 points were plotted.

75 ± 6 nM to 191 ± 18 nM after 15 s, $n = 4$); this response was not affected by a preincubation with 3 μM CRAMP (from 80 ± 11 nM to 236 ± 17 nM, $n = 3$, data not shown). fMLF, MMK-1 and WKYMVm did not affect the increase of the $[Ca^{2+}]_i$ in response to 1 mM ATP. From these results it can be concluded that the inhibition of the response to ATP by CRAMP is not reproduced by specific agonists of FPR or FPRL receptors. Our data also suggest that CRAMP is not an inhibitor of the receptors activated by WKYMVm.

3.4. Effect of CRAMP on the formation of a pore in response to ATP

The sustained activation of the $P2X_7$ receptor eventually provokes the formation of a pore permeant to large ions like ethidium. Once inside the cell, the salt interacts with double-strand nucleic acids and becomes fluorescent [22]. As shown in the upper panel of Fig. 6, the fluorescence emitted by ethidium bromide slightly increased with time in macrophages incubated in control conditions. The slope of the curve was increased about 3-fold by the addition of ATP to the medium. In the next experiments the cells were exposed to 3 μM CRAMP before the addition of 1 mM ATP. The peptide had no effect by itself on the uptake of ethidium bromide but nearly fully blocked the response to ATP (Fig. 6, lower panel). The prolonged activation of $P2X_7$ receptors provokes the release of LDH. The incubations of macrophages with 1 mM ATP for 30 min at 37 °C increased the relase of LDH from 19 ± 1.5% ($n = 11$) to 42.2 ± 2.2% ($n = 10$). By itself 3 μM CRAMP did not affect the release of LDH (20.4 ± 1.8%, $n = 10$) but the peptide inhibited the effect of 1 mM ATP (30.8 ± 3.9%, $n = 6$, $P < 0.05$ when compared to ATP alone). These results suggested that CRAMP inhibited not only the non-specific cation channel coupled to $P2X_7$ receptors but also the formation of a pore by these receptors and the subsequent cell death.

3.5. Effect of CRAMP on the release of oleic acid provoked by extracellular ATP

Purinergic agonists increase the release of oleic acid from peritoneal macrophages: this response is probably secondary to their activation of various phospholipases [29]. As shown in Fig. 7, 1 mM ATP increased the release of oleic acid from macrophages labelled with [^{3}H]oleic acid (from 6.8 ± 0.6% during a 20-min incubation at 25 °C to 12.8 ± 0.8% after a 20-min incubation in the presence of ATP, $n = 9$). By itself CRAMP had no effect on the basal release of oleic acid (6.8 ± 0.8% and 6.0 ± 0.7% in the presence of 1 and 3 μM CRAMP). The peptide inhibited the response to extracellular ATP: the nucleotide only increased the release of [^{3}H]oleic acid to 8.4 ± 0.8% and 8.5 ± 1.0% ($n = 9$) in the presence of respectively 1 and 3 μM CRAMP.

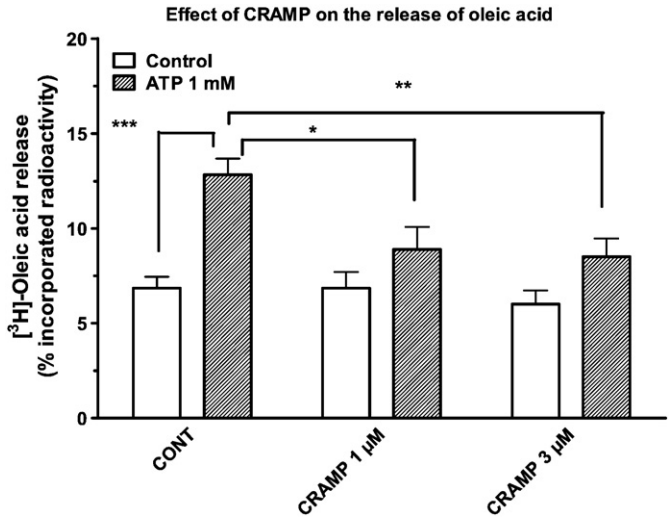

Fig. 7. Effect of CRAMP on the release of [^{3}H]oleic in response to ATP. Murine peritoneal macrophages were prelabelled with [^{3}H]oleic acid and washed as described in Materials and methods. The cells were incubated for 20 min in control conditions or in the presence of 1 mM ATP, 1 or 3 µM CRAMP or in the combined presence of ATP and CRAMP. The results are expressed as the percentage of the total radioactivity incorporated in the cells and are the means ± S.E.M. of 11 (control and 3 µM CRAMP) or 4 experiments (1 µM CRAMP). *P<0.05, **P<0.01, ***P<0.001.

3.6. Effect of CRAMP on the production of ROS in response to extracellular ATP

The production and the release of ROS is a major response of macrophages to extracellular ATP [30]. As shown in Fig. 8, the fluorescence of DCF was stable in macrophages incubated either in control conditions (upper panel) or in the presence of 3 µM CRAMP (lower panel). This result suggested that the fluorescent probe remained in a reduced form when the cells were maintained in basal conditions. The addition of ATP to the medium provoked a linear increase of the fluorescence of DCF (+6364 ± 1191 a.f.u. (n = 10) after a 3-min exposure to ATP) secondary to its oxidation by the ROS produced in response to ATP. A preincubation with 3 µM CRAMP strongly inhibited the response to ATP (+3320 ± 415 a.f.u. after a 3-min exposure to ATP, n = 9, P<0.01 when compared to the fluorescence in the presence of ATP alone).

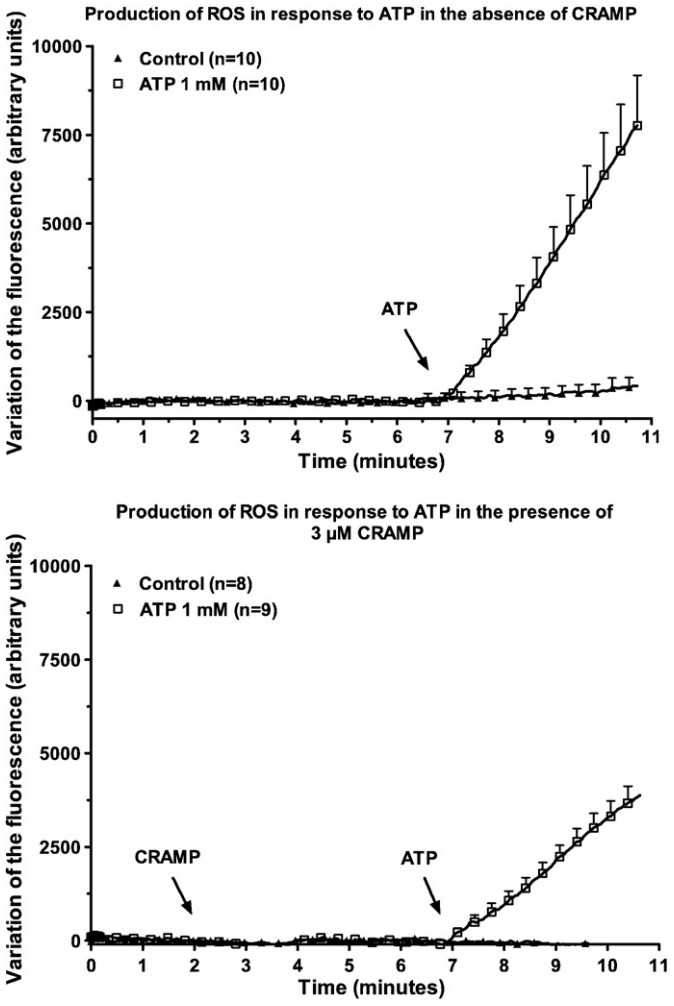

Fig. 8. Effect of CRAMP on the production of ROS in response to ATP. Peritoneal macrophages loaded with DCF were incubated at 25 °C in the presence of 1 mM $CaCl_2$. Two minutes after the start of the assay 3 µM CRAMP was added to the medium (lower panel) or the cells were maintained in control conditions (upper panel). Five minutes later some cells were exposed to 1 mM ATP (squares) and the other cells were incubated in control conditions (triangles). The results are expressed as arbitrary fluorescence units (a.f.u.) and are the means ± S.E.M. of n experiments.

3.7. Effect of CRAMP on the secretion of IL-1β in response to extracellular ATP

$P2X_7$ receptors trigger caspase-1 activation and IL-1β secretion from peritoneal macrophages. After a 20-min incubation with 1 mM ATP the concentration of IL-1β in the medium increased from 411 ± 81 pg /mL (n = 5) to 2634 ± 434 pg/mL (n = 10). CRAMP (3 µM) did not modify the basal release of IL-1β (552 ± 130 pg/mL). CRAMP inhibited the secretion of IL-1β in response to extracellular ATP (1594 ± 195 pg/mL, n = 5, P<0.05 when compared to ATP alone).

3.8. Secondary structure of CRAMP

In a final experiment we examined the secondary structure of CRAMP using ATR-FTIR spectroscopy. These measurements were performed with 5 µg CRAMP or KR-20, the peptide containing the 20 last residues of LL-37 [31]. The spectra of the two peptides were compared with the spectra of myoglobin, as a reference for a predominently α-helical structure, and avidin, as a β-sheet reference structure . As shown in Fig. 9, the spectrum of myoglobin showed two major quasi-symmetrical peaks in the 1500–1800 cm^{-1} range. The peak centered at 1655 cm^{-1} is the amide I signal. The second band at 1545 cm^{-1} is the amide II signal. In the spectrum of avidin a first peak at 1630 cm^{-1} was observed (Fig. 9A, peak 1) This peak had a shoulder around 1650 cm^{-1}. A second peak for avidin was centered around 1530 cm^{-1} (Fig. 9A, peak 2). The spectrum of KR-20 was very similar to the spectrum of myoglobin with two symmetrical peaks at 1656 and 1545 cm^{-1}, suggesting that the peptide had an α-helicoidal secondary structure in aqueous medium. The spectrum of CRAMP was also mostly in favor of an α-helix structure except that the amide I signal was not symmetrical: it had a tail around 1640 cm^{-1} suggesting a slight β-sheet component and a shoulder around 1675 cm^{-1} probably due to a turn (Fig. 9). These initial results led us to suspect that both CRAMP and KR-20 formed predominently an α-helix in our experimental conditions. In a next step the two peptides were deuterated after flushing with nitrogen gas saturated with D_2O. Deuteration is generally used to eliminate a possible contribution of random coil structure (which is very sensitive to deuteration) to the very close alpha helical spectral region (which is less sensitive to deuteration). Deuteration amplified the asymmetry of the amide I peak and an analysis of the deuterated curve revealed the major peak near 1652 cm^{-1} and also two minor peaks centered at 1674 cm^{-1} and 1630 cm^{-1}. The amide II peak for both peptides decreased with time (about −20% after 15 min for KR-20 and −40% for CRAMP). In the same time a peak around 1440 cm^{-1} increased. These results

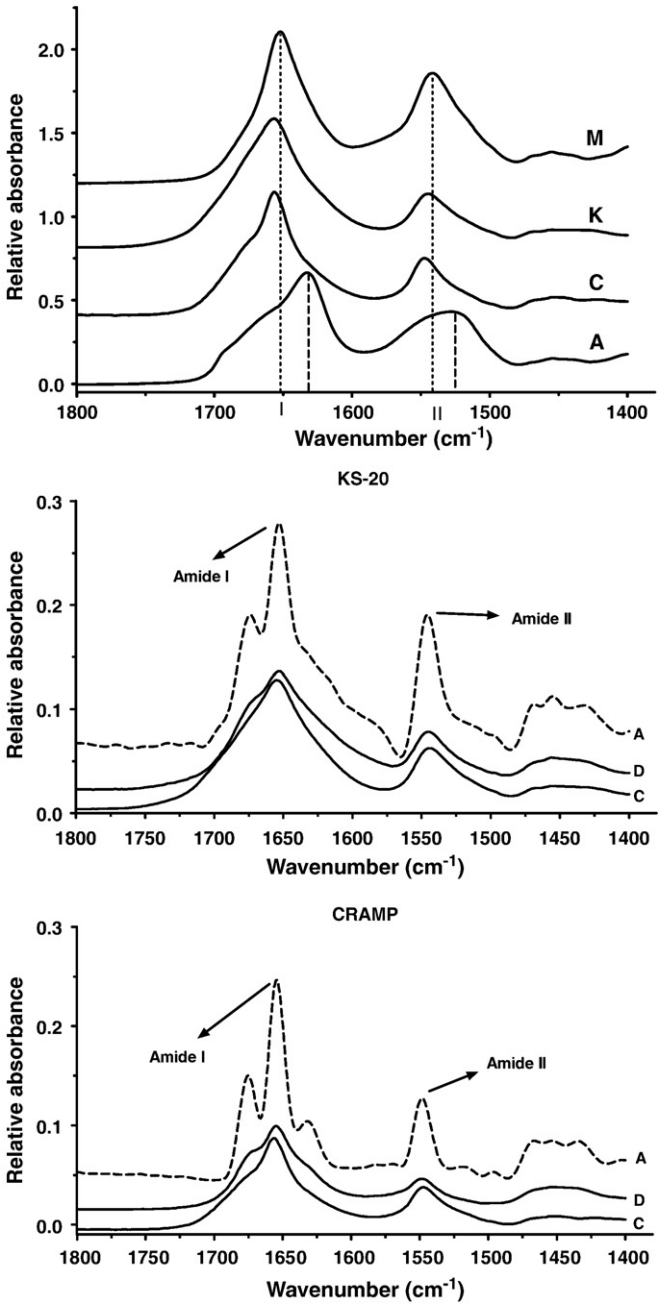

Fig. 9. Infrared-ATR spectra of KR-20 and CRAMP. Upper panel: The spectra of KR-20 (K) and CRAMP (C) were compared to the spectra of avidin (A) and myoglobin (M). Middle and lower panel: The spectra of KR-20 (middle panel) and of CRAMP (lower panel) were measured before (C) or after (D) deuteration. The spectra after deuteration were analyzed using Fourier self-deconvolution (A).

suggested that in an aqueous buffer, KR-20 formed a quasi-perfect α-helical structure while the secondary structure of CRAMP was probably more complex but also formed at least partly an α-helix.

4. Discussion

In this work we show that CRAMP inhibits the sustained increase of the $[Ca^{2+}]_i$, the decrease of the $[K^+]_i$, the uptake of ethidium bromide, the release of LDH, IL-1β and of oleic acid and the production of ROS elicited by extracellular ATP in murine peritoneal macrophages. Macrophages express both P2Y and P2X receptors but the responses to extracellular ATP affected by CRAMP are all mediated by $P2X_7$ receptors [32], suggesting that CRAMP blocks the activation of these purinergic receptors. This is in part confirmed by the experiments performed with macrophages from $P2X_7$-KO mice. In these cells ATP only provoked a transient increase of the $[Ca^{2+}]_i$ confirming that macrophages from KO mice did not express functional $P2X_7$ receptors. The small increase of the $[Ca^{2+}]_i$ was strongly potentiated by ivermectin. This macrolide inhibits the desensitization of $P2X_4$ receptors by blocking the internalization of the receptors [27]. CRAMP had no effect on the increase of the $[Ca^{2+}]_i$ provoked by a combination of ATP and ivermectin, confirming that CRAMP did not interact with the signalling pathway coupled to $P2X_4$ receptors. The selectivity of the effect of CRAMP on $P2X_7$ receptors but not on $P2X_4$ receptors excludes a non-specific effect of CRAMP on the plasma membrane.

LL-37 and CRAMP have been shown to chemoattract neutrophils, T lymphocytes, monocytes or macrophages after binding to FPRL-1/FPR2 [28]. In murine peritoneal macrophages fMLF, an agonist of FPR [14] and MMK-1, a specific agonist of FPRL-1/FPR2 [33] did not increase the $[Ca^{2+}]_i$. WKYMVm, a specific agonist for FPRL-2/FPR3 [34], transiently doubled the $[Ca^{2+}]_i$. This is consistent with the current view that murine macrophages occasionally express FPRL-2/FPR3 [35]. CRAMP had no effect on this response to WKYMVm suggesting that it does not interact with FPRL-2/FPR3. None of the three agonists of the FPR reproduced the inhibition exerted by CRAMP on the increase of the $[Ca^{2+}]_i$ elicited by ATP. These results suggest that FPR do not mediate the inhibition exerted by CRAMP on $P2X_7$ receptors.

This inhibition was unexpected considering that in human macrophages LL-37 mimicked the response to extracellular ATP and increased the secretion of IL-1β. Antagonists of the $P2X_7$ receptor blocked this response, and it was concluded that the $P2X_7$ receptor was activated when human macrophages were incubated in the presence of LL-37 [16]. Several models have been proposed to explain this activation of $P2X_7$ receptors by LL-37. It was initially suggested that LL-37 might increase the permeability of the plasma membrane and provoke the release of intracellular ATP which could have some autocrine effects [16]. LL-37 itself might interact with the extracellular loop of the receptor or with its C-terminal domain after entering the cell [36]. This last hypothesis was recently excluded by Tomasinsig et al. who reported that LL-37 could interact even with a $P2X_7$ receptor lacking the intracellular C-terminal domain [37]. These authors also observed that the capacity to stimulate $P2X_7$ receptors varied among cathelicidin-derived peptides. The LL-37 from orangutan and from gibbon which, like the human LL-37, can form an α-helix not only in organic medium but also in aqueous solutions, stimulated the $P2X_7$ receptors. The LL-37 from macaque or from leaf monkey which have a lower structuring capacity did not interact with the $P2X_7$ receptors. These results led Tomasinsig et al. to conclude that the ability of antimicrobial peptides to react with $P2X_7$ receptors was related to their ability to form an amphipathic α-helix in aqueous solution [37]. LL-37 and CRAMP share major structural properties: they lack cysteine residues and are small cationic peptides with a net positive charge of 6 for both peptides and a high content of hydrophobic residues (35% for LL-37 and 29% for CRAMP). They also share the capacity to form an amphipatic α-helix in organic solvents. Using ATR-FTIR spectroscopy we have studied the secondary structure of CRAMP and of the C-terminal eicosapeptide of LL-37, KR-20 (this peptide contains most of the alpha-helical structure of LL-37) [38]. These peptides were dissolved in a 2 mM HEPES buffer (pH 7.4). It has been demonstrated that ATR-FTIR can provide important information on the secondary structure of a protein and on its modifications after interaction with a ligand, a lipid or another protein [24]. These informations can be obtained by the analysis of the amide I peak (corresponding to the C=O vibration) and the amide II peak (corresponding to the N–H deformation). These peaks are observed at different wavelengths when present in a random coil structure, or in an α-helix, or in a β-sheet. The spectra of the two peptides revealed that the amide I and II peaks were centered at wavelengths

corresponding to α-helices. The capacity to exchange hydrogen for deuterium in the N–H group is also related to the relative content of secondary structures in the protein: this exchange is very slow in a well-structured region of a protein or a peptide. The height of the amide I and II peaks in the presence of D_2O vapor can thus be used as an index of the relative structural compactness of the protein. The decrease of these peaks was rather small suggesting that the two peptides had well-defined secondary structures rather than random structures. Deuteration modified the shape of the amide I peak and exacerbated the shoulders observed around 1630 and 1670 cm^{-1}, especially for CRAMP. From these results we can conclude that KR-20 forms mostly an α-helix in an aqueous buffer. The structure of CRAMP seems more complex combining both some α-helix and a turn. The presence of two prolyl residues in the C-terminal region of CRAMP (positions 30 and 32) might account for this turn. Our results are at variance with the previous observations of Yu et al. [39]. Using circular dichroism analysis and NMR spectroscopy these authors reported that in aqueous solutions CRAMP adopted a random coil structure but that it formed an α-helix in membrane mimetics environments. The discrepancy between their results and ours might be explained by the fact that peptides with different primary structures were used in the two studies. There is 85% similarity between the two peptides. We used a peptide with 34 amino acids. Its sequence has been reported by Pestonjamasp et al. [40], and it corresponds to the peptide registered as CRAMP in the database for antimicrobial peptides (access number AP00281) [41]. The peptide used by Yu et al. has 38 amino acids: it lacks the C-terminal Q but has a pentapeptide extension (ISRLA) at the N-terminus. The peptide of Yu et al. has also an extra positive charge at neutral pH (+7) and has a higher proportion of hydrophobic residues (34%). Ten of these hydrophobic residues are located on the same side of a potential α-helix in their peptide and only six residues have a similar position in our CRAMP. These differences in the primary structure of the two peptides might account for their distinct conformations in water. Thus both LL-37 and CRAMP can form an α-helix in aqueous buffer and interact with $P2X_7$ receptors but LL-37 is an agonist on $P2X_7$ receptors from man and CRAMP is an antagonist on murine $P2X_7$ receptors. The two peptides have a different index of binding potential: 2.99 kcal/mol for LL-37 and only 1.74 kcal/mol for CRAMP [41]. This difference in energy could account for the ability of LL-37 to switch the receptor in an active conformation. However this hypothesis cannot explain why LL-37 blocked the responses coupled to $P2X_7$ receptors in mouse submandibular glands [17]. The best explanation for these results would be that not only the peptides but also the receptors themselves contribute to the difference in the interaction between antimicrobial peptides and $P2X_7$ receptors. Mouse and man $P2X_7$ receptors share 80% homology but they diverge with respect to their sensitivity towards agonists (specially benzoyl-ATP) or antagonists (specially isoquinolone derivatives) [42]. It is thus reasonable to conceive that $P2X_7$ receptors from mouse and man have different responses to antimicrobial peptides.

In conclusion our results with the mouse model (CRAMP and murine macrophages) confirm that the antimicrobial peptide and the receptor can interact but clearly establish that this interaction is not always positive and that antimicrobial peptides are thus not universal agonists of $P2X_7$ receptors.

References

[1] M. Zasloff, Antimicrobial peptides in health and disease, N. Engl. J. Med. 347 (2002) 1199–1200.

[2] M. Zanetti, R. Gennaro, D. Romeo, Cathelicidins: a novel protein family with a common proregion and a variable C-terminal antimicrobial domain, FEBS Lett. 374 (1995) 1–5.

[3] M. Zanetti, Cathelicidins, multifunctional peptides of the innate immunity, J. Leukoc. Biol. 75 (2004) 39–48.

[4] G.H. Gudmundsson, B. Agerberth, J. Odeberg, T. Bergman, B. Olsson, R. Salcedo, The human gene FALL39 and processing of the cathelin precursor to the antibacterial peptide LL-37 in granulocytes, Eur. J. Biochem. 238 (1996) 325–332.

[5] J. Johansson, G.H. Gudmundsson, M.E. Rottenberg, K.D. Berndt, B. Agerberth, Conformation-dependent antibacterial activity of the naturally occurring human peptide LL-37, J. Biol. Chem. 273 (1998) 3718–3724.

[6] S.M. Travis, N.N. Anderson, W.R. Forsyth, C. Espiritu, B.D. Conway, E.P. Greenberg, P.B. McCray, R.I. Lehrer, M.J. Welsh, B.F. Tack, Bactericidal activity of mammalian cathelicidin-derived peptides, Infect. Immun. 68 (2000) 2748–2755.

[7] M. Golec, Cathelicidin LL-37: LPS-neutralizing, pleiotropic peptide, Ann. Agric. Environ. Med. 14 (2007) 1–4.

[8] B. Agerberth, J. Charo, J. Werr, B. Olsson, F. Idali, L. Lindbom, R. Kiessling, H. Jörnvall, H. Wigzell, G.H. Gudmundsson, The human antimicrobial and chemotactic peptides LL-37 and alpha-defensins are expressed by specific lymphocyte and monocyte populations, Blood 96 (2000) 3086–3093.

[9] J.D. Heilborn, M.F. Nilsson, G. Kratz, G. Weber, O. Sørensen, N. Borregaard, M. Ståhle-Bäckdahl, The cathelicidin anti-microbial peptide LL-37 is involved in re-epithelialization of human skin wounds and is lacking in chronic ulcer epithelium, J. Invest. Dermatol. 120 (2003) 379–389.

[10] R. Koczulla, G. von Degenfeld, C. Kupatt, F. Krötz, S. Zahler, T. Gloe, K. Issbrücker, P. Unterberger, M. Zaiou, C. Lebherz, A. Karl, P. Raake, A. Pfosser, P. Boekstegers, U. Welsch, P.S. Hiemstra, C. Vogelmeier, R.L. Gallo, M. Clauss, R. Bals, An angiogenic role for the human peptide antibiotic LL-37/hCAP-18, J. Clin. Invest. 111 (2003) 1665–1672.

[11] M. Gough, R.E. Hancock, N.M. Kelly, Antiendotoxin activity of cationic peptide antimicrobial agents, Infect. Immun. 64 (1996) 4922–4927.

[12] K. Kandler, R. Shaykhiev, P. Kleemann, F. Klescz, M. Lohoff, C. Vogelmeier, R. Bals, The anti-microbial peptide LL-37 inhibits the activation of dendritic cells by TLR ligands, Int. Immunol. 18 (2006) 1729–1736.

[13] G.S. Tjabringa, J. Aarbiou, D.K. Ninaber, J.W. Drijfhout, O.E. Sørensen, N. Borregaard, K.F. Rabe, P.S. Hiemstra, The antimicrobial peptide LL-37 activates innate immunity at the airway epithelial surface by transactivation of the epidermal growth factor receptor, J. Immunol. 171 (2003) 6690–6696.

[14] Y. Le, Y. Yang, Y. Cui, H. Yazawa, W. Gong, C. Qiu, J.M. Wang, Receptors for chemotactic formyl peptides as pharmacological targets, Int. Immunopharmacol. 2 (2002) 1–13.

[15] N. Mookherjee, D.N.D. Lippert, P. Hamill, R. Falsafi, A. Nijnik, J. Kindrachuk, J. Pistolic, J. Gardy, P. Miri, M. Naseer, L.J. Foster, R.E.W. Hancock, Intracellular receptor for human host defense peptide LL-37 in monocytes, J. Immunol. 183 (2009) 2688–2696.

[16] A. Elssner, M. Duncan, M. Gavrilin, M.D. Wewers, A novel $P2X_7$ receptor activator, the human cathelicidin-derived peptide LL-37, induces IL-1 beta processing and release, J. Immunol. 72 (2004) 4987–4994.

[17] S. Pochet, S. Tandel, S. Querriére, M. Tre-Hardy, M. Garcia-Marcos, M. De Lorenzi, M. Vandenbranden, A. Marino, M. Devleeschouwer, J.P. Dehaye, Modulation by LL-37 of the responses of salivary glands to purinergic agonists, Mol. Pharmacol. 69 (2006) 2037–2046.

[18] R.L. Gallo, K.J. Kim, M. Bernfield, C.A. Kozak, M. Zanetti, L. Merluzzi, R. Gennaro, Identification of CRAMP, a cathelin-related antimicrobial peptide expressed in the embryonic and adult mouse, J. Biol. Chem. 272 (1997) 13088–13093.

[19] S. Pochet, M. Garcia-Marcos, M. Seil, A. Otto, A. Marino, J.P. Dehaye, Contribution of two ionotropic purinergic receptors to ATP responses in submandibular gland ductal cells, Cell. Signal. 19 (2007) 2155–2164.

[20] R.M. McCarron, D.K. Goroff, J.E. Luhr, M.A. Murphy, H.B. Herscowitz, Methods for the collection of peritoneal and alveolar macrophages, Methods Enzymol 108 (1984) 274–284.

[21] G. Grynkiewicz, M. Poenie, R.Y. Tsien, A new generation of Ca^{2+} indicators with greatly improved fluorescence properties, J. Biol. Chem. 260 (1985) 3440–3450.

[22] E. Alzola, N. Chaïb, S. Pochet, E. Kabré, A. Marino, J.P. Dehaye, Modulation by propranolol of the uptake of ethidium bromide by rat submandibular acinar cells exposed to a $P2X_7$ agonist or to maitotoxin, Cell. Signal. 13 (2001) 465–473.

[23] M. Seil, U. Fontanils, I.G. Etxebarria, S. Pochet, M. Garcia-Marcos, A. Marino, J.P. Dehaye, Pharmacological evidence for the stimulation of NADPH oxidase by $P2X_7$ receptors in mouse submandibular glands, Purinergic Signal. 4 (2008) 347–355.

[24] C. Vigano, L. Manciu, F. Buyse, E. Goormaghtigh, J.M. Ruysschaert, Attenuated total reflection IR spectroscopy as a tool to investigate the structure, orientation and tertiary structure changes in peptides and membrane proteins, Biopolymers 55 (2000) 373–380.

[25] E. Goormaghtigh, J.M. Ruysschaert, V. Raussens, Evaluation of the information content in infrared spectra for protein secondary structure determination, Biophys. J. 89 (2006) 2946–2957.

[26] R. Coutinho-Silva, D.M. Ojcius, D.C. Gorecki, P.M. Persechini, R.C. Bisaggio, A.N. Mendes, J. Marks, G. Burnstock, P.M. Dunn, Multiple P2X and P2Y receptor subtypes in mouse J774, spleen and peritoneal macrophages, Biochem. Pharmacol. 69 (2005) 641–655.

[27] E. Toulmé, F. Soto, M. Garret, E. Boué–Grabot, Functional properties of internalization-deficient $P2X_4$ receptors reveal a novel mechanism of ligand-gated channel facilitation by ivermectin, Mol. Pharmacol. 69 (2006) 576–587.

[28] K. Kurosaka, Q. Chen, F. Yarovinsky, J.J. Oppenheim, D. Yang, Mouse cathelin-related antimicrobial peptide chemoattracts leukocytes using formyl peptide receptor-like 1/mouse formyl peptide receptor-like 2 as the receptor and acts as an immune adjuvant, J. Immunol. 174 (2005) 6257–6265.

[29] M. Garcia-Marcos, S. Pochet, A. Marino, J.P. Dehaye, $P2X_7$ and phospholipids signalling: the search of the "missing link" in epithelial cells, Cell. Signal. 18 (2006) 2098–2104.

[30] Z.A. Pfeiffer, A.N. Guerra, L.M. Hill, M.L. Gavala, U. Prabhu, M. Aga, D.J. Hall, P.J. Bertics, Nucleotide receptor signaling in murine macrophages is linked to reactive oxygen species generation, Free Radic. Biol. Med. 42 (2007) 1506–1516.

[31] M. Murakami, B. Lopez-Garcia, M. Braff, R.A. Dorschner, R.L. Gallo, Postsecretory processing generates multiple cathelicidins for enhanced topical antimicrobial defense, J. Immunol. 172 (2004) 3070–3077.

[32] A.M. Surprenant, R.A. North, Signaling at Purinergic P2X Receptors, Annu. Rev. Physiol. 71 (2008) 333–359.
[33] J.Y. Hu, Y. Le, W. Gong, N.M. Dunlop, J.L. Gao, P.M. Murphy, J.M. Wang, Synthetic peptide MMK-1 is a highly specific chemotactic agonist for leukocyte FPRL1, J. Leukoc. Biol. 70 (2001) 155–161.
[34] H.K. Kang, H.Y. Lee, M.K. Kim, K.S. Park, Y.M. Park, J.Y. Kwak, Y.S. Bae, The synthetic peptide Trp-Lys-Tyr-Met-Val-D-Met inhibits human monocyte-derived dendritic cell maturation via formyl peptide receptor and formyl peptide receptor-like 2, J. Immunol. 175 (2005) 685–692.
[35] T. Devosse, A. Guillabert, N. D'Haene, A. Berton, P. De Nadai, S. Noel, M. Brait, J.D. Franssen, S. Sozzani, I. Salmon, M. Parmentier, Formyl peptide receptor-like 2 is expressed and functional in plasmacytoid dendritic cells, tissue-specific macrophage subpopulations, and eosinophils, J. Immunol. 182 (2009) 4974–4984.
[36] M.D. Wewers, A. Sarkar, $P2X_7$ receptor and macrophage function, Purinergic Signal 5 (2009) 189–195.
[37] L. Tomasinsig, C. Pizzirani, B. Skerlavaj, P. Pellegatti, S. Gulinelli, A. Tossi, F. Di Virgilio, M. Zanetti, The human cathelicidin LL-37 modulates the activities of the $P2X_7$ receptor in a structure-dependent manner, J. Biol. Chem. 283 (2008) 30471–30481.
[38] K. Yu, K. Park, S.-W. Kang, S.Y. Shin, K.-S. Hahm, Y. Kim, Solution structure of a cathelicidin-derived antimicrobial peptide, CRAMP as determined by NMR spectroscopy, J. Peptide Res. 60 (2002) 1–9.
[39] V.K. Pestonjamasp, K.H. Huttner, R.L. Gallo, Processing site and gene structure for the murine antimicrobial peptide CRAMP, Peptides 22 (2001) 1643–1650.
[40] G. Wang, X. Li, Z. Wang, APD2: the updated antimicrobial peptide data base and its application in peptide design, Nucleic Acids Res 37 (2009) D933–D937.
[41] I.P. Chessell, J. Simon, A.D. Hibell, A.D. Michel, E.A. Barnard, P.P. Humphrey, Cloning and functional characterisation of the mouse $P2X_7$ receptor, FEBS Lett. 13 (1998) 26–30.
[42] M.T. Young, P. Pelegrin, A. Surprenant, Surprenant, Amino acid residues in the P2X7 receptor that mediate differential sensitivity to ATP and BzATP, Mol Pharmacol. 71 (2007) 92–100.